Published in final edited form as:
Biomaterials. 2011 February ; 32(6): 1583–1590. doi:10.1016/j.biomaterials.2010.10.056.

Cell Infiltration and Growth in a Low Density, Uncompressed Three-Dimensional Electrospun Nanofibrous Scaffold

Bryan A. Blakeney[1,a], **Ajay Tambralli**[1,a], **Joel M. Anderson**[a], **Adinarayana Andukuri**[a], **Dong-Jin Lim**[a], **Derrick R. Dean**[b], and **Ho-Wook Jun**[a,*]

[a]Department of Biomedical Engineering, University of Alabama at Birmingham, 1825 University Boulevard, Birmingham, AL 35294

[b]Department of Materials Science and Engineering, University of Alabama at Birmingham, 1530 3rd Avenue South, Birmingham, AL 35294

Abstract

A limiting factor of traditional electrospinning is that the electrospun scaffolds consist entirely of tightly packed nanofiber layers that only provide a superficial porous structure due to the sheet-like assembly process. This unavoidable characteristic hinders cell infiltration and growth throughout the nanofibrous scaffolds. Numerous strategies have been tried to overcome this challenge, including the incorporation of nanoparticles, using larger microfibers, or removing embedded salt or water-soluble fibers to increase porosity. However, these methods still produce sheet-like nanofibrous scaffolds, failing to create a porous three-dimensional scaffold with good structural integrity. Thus, we have developed a three-dimensional cotton ball-like electrospun scaffold that consists of an accumulation of nanofibers in a low density and uncompressed manner. Instead of a traditional flat-plate collector, a grounded spherical dish and an array of needle-like probes were used to create a Focused, Low density, Uncompressed nanoFiber (FLUF) mesh scaffold. Scanning electron microscopy showed that the cotton ball-like scaffold consisted of electrospun nanofibers with a similar diameter but larger pores and less dense structure compared to the traditional electrospun scaffolds. In addition, laser confocal microscopy demonstrated an open porosity and loosely packed structure throughout the depth of the cotton ball-like scaffold, contrasting the superficially porous and tightly packed structure of the traditional electrospun scaffold. Cells seeded on the cotton ball-like scaffold infiltrated into the scaffold after 7 days of growth, compared to no penetrating growth for the traditional electrospun scaffold. Quantitative analysis showed approximately a 40% higher growth rate for cells on the cotton ball-like scaffold over a 7 day period, possibly due to the increased space for in-growth within the three-dimensional scaffolds. Overall, this method assembles a nanofibrous scaffold that is more advantageous for highly porous interconnectivity and demonstrates great potential for tackling current challenges of electrospun scaffolds.

[*]Corresponding author: Department of Biomedical Engineering, 806 Shelby Building, 1825 University Boulevard, Birmingham, AL 35294, United States. Tel.: +1 205 996 6938; fax: +1 205 975 4919. hwjun@uab.edu (H.W. Jun)..
[1]These authors contributed equally.

Keywords

Electrospinning; Scaffold; Biomimetic material; Extracellular matrix (ECM); Nanofibers; Tissue Engineering

1. Introduction

Traditional electrospinning produces flat, highly interconnected scaffolds consisting of densely packed nanofibers. These electrospun scaffolds can support the adhesion, growth, and function of various cell types, while also promoting their maturation into specific tissue lineages, such as bone [1–3], cartilage [4], tendons, ligaments [5], skin [6,7], neurons [8], liver [9], smooth muscle [10], striated muscle [11,12], and even cornea [13]. In addition, the morphology of electrospun nanofibrous scaffolds is highly tunable by simply modifying any number of fabrication parameters, such as concentration of polymer solution or voltage between nozzle and collector [14]. This is very advantageous for tissue engineering systems because it has been shown that the fiber diameter [15], pore size [16], and even solvent used [17] affect cellular response to electrospun biomaterials. However, a major limitation of traditional electrospun scaffolds is that they have tightly packed layers of nanofibers with only a superficially porous network, resulting in confinement to sheet-like formations only. This unavoidable characteristic restricts cell infiltration and growth through the scaffolds. Thus, it is imperative to develop an innovative strategy capable of fabricating an electrospun scaffold with a stable three dimensional structure, while exhibiting nanofibrous morphologies and deep, interconnected pores. Such a scaffold would better mimic the configuration of native extracellular matrix (ECM), thereby maximizing the likelihood of long-term cell survival and generation of functional tissue within a biomimetic environment.

The techniques used for traditional electrospinning employ a static, flat-plate collector placed at a set distance away from a charged nozzle containing a polymer solution. The resulting electrospun scaffolds are composed of nanofibrous layers arranged in a tightly packed conformation, which allows cellular growth and infiltration near the superficial surface but not deep within the internal structure. Many potential solutions have been investigated to improve this scaffold deficiency; however, the paradoxical nature of the electrospinning process works against achieving an ideal formation that allows for both good cell attachment and deep cellular infiltration. Specifically, as the fiber diameter decreases to the nanoscale range for optimal cell attachment, the porosity decreases as well, thereby preventing deep cellular infiltration that is most easily overcome by reverting back to microscaled fiber diameters [18]. This drawback has previously discouraged exclusively electrospun scaffolds, and has led to exploration of other electrospun nanofiber uses, such as coatings for more porous scaffold material including microfibers [19].

Of the previous methods explored for improving cellular infiltration, one common strategy utilizes salts dissolved in the polymer solution to create specific pore sizes throughout the scaffold by leaching out the particulates after electrospinning [20,21]. This forms porous spaces in the scaffold; however, the spaces act as a divider for creating separate layers within the scaffold, much like layering multiple scaffolds [22,23], which does not provide uniform morphology and stability. Another previous strategy involves co-electrospinning the desired polymer with an easily water-soluble material and then dissolving it out [24]. This removes continuous sections within the scaffold; however, the sudden removal of these fibers causes reorganization and contraction of the fibers, which often leads to blockage of the newly created pores [16] and collapses the mesh network of the scaffold [25]. Another approach is to electrospray hydrogels into the scaffold as it is being formed [25]. This creates pockets of hydrogels through which cells can infiltrate deep into the scaffold.

However, this method does not produce a true three-dimensional scaffold with interconnected pores because the sprayed hydrogel is difficult to disperse evenly, again leading to a non-uniform scaffold that is unlikely to induce consistent growth throughout. In addition, using rotating drums as collectors creates a hollow shape; however, it still collects nanofibers as tightly packed layers [26].

The main reason that the above methods do not completely overcome the current challenges of electrospun scaffolds is because they are adaptations of the traditional electrospinning technique. Thus, for all current modification methods, the creation of an electrospun nanofiber involves a bead of polymer solution being drawn into a nanoscale fiber due to the applied electric charge. As the nanofiber is dispersed, it then follows the electric potential gradient from the highest (charged nozzle) to the lowest (grounded voltage source), leading to deposition on the nearby collector. As a result of this force, subsequent fiber layers are deposited one on top of the other as two dimensional formations that ultimately form a densely packed structure. Therefore, even though each deposited layer can be viewed as having pores within a planar, two dimensional space, these pores do not continue into the cross-section orthogonal to the layers (i.e. depth of the scaffold), limiting cellular infiltration to only the superficial layers.

Overall, all current strategies to create electrospun scaffolds collect nanofibers in an unfocused, planar manner, which causes subsequent layers to adopt a densely packed network and prevents the formation of three dimensional structures with good stability. Therefore, to overcome these obstacles, we hypothesize that electrospun scaffolds can be fabricated as three dimensional structures if the nanofibers are allowed to accumulate in a more open space that still maintains a focused shape, without forcing the fibers to deposit side-by-side. In this manuscript, we demonstrate an innovative strategy for creating a Focused, Low density, and Uncompressed nanoFibrous (FLUF) mesh by using a collection system consisting of an array of metal probes embedded in a non-conductive spherical dish. This encourages the electrospun nanofibers to intertwine and accumulate in the air between the probes, while the spherical dish focuses them into a constrained area. This combination results in the electrospun nanofibers adopting a shape similar to a cotton ball with excellent three dimensional structural stability.

2. Materials and Methods

2.1 Material fabrication

2.1.1 Electrospinning traditional flat-plate electrospun scaffolds—Poly-e-caprolactone (PCL) pellets (M_n: 80,000; Sigma Aldrich, St. Louis, MO) were dissolved at a ratio of 225 mg/ml in a solvent solution of 1:1 (v: v) chloroform and methanol under constant stirring until the mixture was clear, viscous, and homogenous. PCL solution was poured into a syringe capped with a 25 gauge blunt-tipped needle nozzle. The syringe was loaded into a syringe pump (KD Scientific, Holliston, MA) with a set flow rate of 1.0 ml/hr. The flat-plate electrospun scaffolds were then fabricated by traditional methodology as previously described [27]. Briefly, the nozzle was placed 28 cm from a grounded, flat sheet of aluminum foil and attached to the positive terminal of a high voltage generator (Gamma High-Voltage Research, Ormond Beach, FL). A voltage of +21 kV was then applied 1 mm from the needle opening, and the scaffold was electrospun as a sheet onto the grounded collector.

2.1.2 Electrospinning cotton ball-like electrospun scaffolds—Similar to traditional electrospinning, PCL pellets were dissolved at a ratio of 75 mg/ml in a solvent solution of 1:1 (v: v) chloroform and methanol and transferred to a syringe chamber. The filled syringe fitted with a 25 gauge blunt-tipped needle nozzle was then placed into a

syringe pump with a set flow rate of 2.0 ml/hr and at a distance of 15 cm from the front plane of the collector. The nozzle was attached to the positive terminal of a high voltage generator through which a voltage of +15 kV was applied 1 mm from the needle opening, and the three dimensional electrospun scaffold was fabricated onto a custom-made collector.

The collector for the cotton ball-like electrospun scaffolds was specially crafted by embedding an array of 1.5 inch long stainless steel probes in a spherical foam dish (diameter: 8 in., shell thickness: 0.125 in.; Fibre Craft, Niles, IL) backed by a stainless steel lining to provide an electrical ground. The needles were placed at 2 inch intervals radiating from the center of the dish in five equidistant directions. The nanofibers were allowed to accumulate throughout the electrospinning process and then removed with a glass rod.

2.2 Scaffold characterization

2.2.1 Scanning electron microscope (SEM) imaging—The ePCL scaffolds were mounted on an aluminum stub and sputter coated with gold and palladium. A Philips SEM 510 (FEI, Hillsboro, OR) at an accelerating voltage of 20 kV was used to image the scaffolds, and the fiber diameters were measured using GIMP 2.6 for Windows.

2.2.2 Confocal microscope imaging—To visually contrast nanofiber network organization in the traditional flat-plate electrospun scaffold with the cotton ball-like electrospun scaffold, scaffolds were incubated in 4',6-diamidino-2-phenylindole (DAPI; Invitrogen, Carlsbad, CA) for 4 hours. Scaffolds were then imaged using a Zeiss LSM 710 Confocal Laser Scanning Microscope (Thornwood, NY) and analyzed using Zen 2009 software. Since DAPI is strongly attracted to the hydrophobic PCL, the fluorescence clearly illuminated the nanofibrous structures of the scaffolds.

2.3 Cell culturing

INS-1 (832/13) cells, a kind gift from Dr. John A. Corbett (Department of Biochemistry, Medical College of Wisconsin, Milwaukee, WI), were cultured in RPMI-1640 media (Invitrogen) supplemented with 10% fetal bovine serum (FBS, Atlanta Biologicals, Lawrenceville, GA), 2 mM L-glutamine, 10 mM HEPES, 1 mM sodium pyruvate, and 55 μM 2-mercaptoethanol (Invitrogen). Cells were expanded to 80–90% confluency under normal culture conditions (37 °C, 95% relative humidity, 5% CO_2) before seeding on the electrospun scaffolds.

The traditional flat-plate ePCL scaffolds were cut into 0.5 cm discs and placed in 96-well plates according to a method described previously [27]. The size of the cotton ball-like ePCL scaffolds were normalized to a 0.5 cm diameter by trimming with a sterile razor and then placed in a 96-well plate. Sterilization was performed by soaking the electrospun scaffolds in a solution of 70% ethanol and 30% phosphate buffered saline (PBS) for 12 hours under sterile conditions, followed by a serial dilution in PBS over 6 hours, and a final soaking in PBS for 12 hours. All scaffolds were then immersed overnight in the media formulation specified above to allow for protein adsorption.

Prior to cell seeding, excess cell culture media from the overnight soaking were removed for all scaffolds. To study cellular infiltration into the scaffolds and measure cellular proliferation, a cell suspension of 64,000 INS-1 cells was added to each scaffold. The scaffolds were incubated for 2 hours in a humidified incubator and then transferred to 48 well tissue culture plates. An additional 400 μl media were added to each well, and the media was changed every 48 hours. Cellular behavior was analyzed by collecting the scaffolds after 1, 3, and 7 days.

2.4 Histology

To quantify the extent of cellular infiltration, scaffolds were removed from media at the appropriate time points and fixed in formalin overnight. They were then soaked in a 20% sucrose solution, which was exchanged with a 50% sucrose solution 24 hours later. After soaking overnight, the scaffolds were embedded in Histo-Prep embedding medium (Fisher Scientific, Pittsburgh, PA) and snap frozen in liquid nitrogen. The resulting blocks were cut into 20 μm sections using a Microm HM 505E Cryostat with CryoJane Tape-Transfer (Instrumedics, Richmond, IL), and mounted onto Superfrost/Plus microscope slides (Fisher Scientific). To visualize cellular nuclei and cytoplasm, the sections were stained with Hemotoxylin and Eosin dyes (American MasterTech Sci., Lodi, CA). Images were then taken using a Nikon eclipse TE2000-S microscope (Melville, NY) and analyzed using NIS-elements AR 2.30 software.

2.5 Cell proliferation analysis

At the specified time points, cellular proliferation was quantified by using the cell counting kit-8 reagent (CCK-8; Dojindo Molecular Technologies, Rockville, MD) per manufacturer's instructions. Briefly, at each time point, the CCK-8 reagent was added to the specified well in a 1:10 ratio of the total cell culture volume and incubated for 4 hours in a humidified incubator. Each sample was stored in a 4°C fridge until all time points were collected. The absorbance (450 nm) for all samples was measured together using a microplate reader (Synergy HK, BIO-TEK Instruments, Winooski, VT), and the cell number was calibrated against absorbance standards of known cell concentrations.

2.6 Statistical analysis

All experiments were performed in quadruplicate at least three independent times, and the results presented are representative data sets. All values were expressed as means ± standard deviations. All data were compared with one-way ANOVA tests using SPSS software. Tukey multiple comparisons test was performed to evaluate significant differences between pairs. A value of $p < 0.05$ was considered statistically significant.

3. Results and Discussion

The increasing number of roles for synthetic biomaterials in tissue engineering has precipitated new strategies for creating extracellular matrix (ECM) mimicking microenvironments. Among the many biomaterial fabrication methods currently in use, electrospinning has repeatedly been shown to produce biocompatible polymer scaffolds for a variety of applications [28,29]. Electrospinning is particularly attractive because it is a versatile and cost-effective method to repeatedly fabricate nanofibrous scaffolds using synthetic means. However, one limiting factor of the existing electrospinning methods is an inability to simultaneously incorporate nanofibrous morphologies, while still maintaining deep interconnected pores within a stable three dimensional network structure. This presents a significant obstacle for cellular infiltration and growth deep into the scaffolds, limiting the potential of electrospun scaffolds. Thus, there is a critical need for new transformative electrospinning strategies that provide an ECM mimicking microenvironment for cell based tissue engineering applications. Therefore, in this study, we developed an electrospun scaffold that incorporates a 1) three dimensional, cotton ball-like structure, 2) loosely packed, uninterrupted mesh of nanofibers, 3) deep, interconnected pores in all three dimensions, and 4) good structural stability.

The basic method to electrospin polymer fibers is to place a grounded collector near a charged syringe nozzle, which contains a conductive polymer solution. As the applied voltage is increased, the solution overcomes the frictional forces, resulting in a spinning jet

of polymer fluid being ejected from the needle. This ejected solution evaporates as it travels over the projected distance, depositing a mesh of fibers on the collector (Figure 1a). The resulting fiber characteristics are largely determined by the solution viscosity, flow rate, and distance between nozzle and collector. (Low viscosities, low flow rates, and large distances generally result in smaller diameters.) However, the overall scaffold characteristics are largely determined by the collector.

On a traditional flat-plate collector, the grounded charge is spread uniformly over a large area. As a result, a group of fibers is deposited side-by-side in one layer, and each subsequent layer is deposited on top of the existing layers. However, each layer is still strongly attracted to the grounded collector, thus compressing the layers below. This creates a flat, sheet-like structure with densely packed fiber layers and superficial, planar pores, which do not continue deep into the scaffold (Figure 2a). While the accumulated fiber layers do provide a thickness to the scaffold, the lack of space between adjacent layers essentially creates a two dimensional scaffold, especially since cellular growth and infiltration are limited to the superficial layers.

Therefore, to create an electrospun scaffold with nanofibrous morphologies and deep, interconnected pores incorporated within a more realized three dimensional structure, we replaced the traditional collector with a non-conductive spherical dish that has an array of embedded metal probes (Figure 1b). This innovative arrangement evenly dispersed and concentrated the grounded charge on the probes. The probes are then able to collect the nanofibers between them in mid-air, and the lack of a uniform charge throughout the collector allows nanofiber layers to settle next to the previously deposited layers without compressing the scaffold. In addition, the spherical dish helps collect the nanofibers in a focused area, thereby accumulating them as a fluffy, three dimensional structure with good stability (Figure 2b).

Comparing Figures 2a and 2b, it is clear that modifying the collector system has a dramatic influence on overall scaffold characteristics. As a result of the uniformly concentrated charge of the traditional collector, the generated scaffold has a very tightly packed structure assembled as in a flat, sheet-like arrangement. In contrast, the spherical dish and metal array collector creates a Focused, Low density, and Uncompressed nanoFibrous (FLUF) mesh with tremendous three dimensional depth. Thus, the collector provides an alternative strategy for overcoming one of the current challenges facing electrospinning fabrication, as new scaffolds were created with a stable, interconnected nanofibrous architecture in multiple planes. Herein, we have designated these new three dimensional assemblies as FLUF scaffolds, which very closely resemble the macrostructure of a cotton ball (Figure 2c). As an added benefit, the cotton ball-like electrospun scaffolds generated for this study took less than 20 minutes to accumulate, whereas it typically takes many hours, maybe even days, to collect a similarly dimensioned scaffold using the traditional fabrication method.

Poly (ε-caprolactone) (PCL) was chosen as the model polymer for this study because it is biocompatible and been FDA approved for use in biomedical applications. Furthermore, PCL can be readily electrospun into nanofibers (ePCL), which can support the growth of chondrocytes, skeletal muscle cells, smooth muscle cells, endothelial cells, fibroblasts, and human mesenchymal stem cells [10,15,27,30–35]. For this study, we evaluated the biological response of the ePCL electrospun scaffolds with a rat insulinoma INS-1 (832/13) cells (INS-1 cells) cell line. INS-1 cells are a very robust cell line that allow for quick and easily obtained biological analysis. Furthermore, this cell line was developed to mimic β-cell function [36–38], which has great utility for studying pancreatic tissue engineering applications, a rapidly emerging area of interest. Thus, to accurately compare nanofiber characteristics and cellular performance in this study, PCL was electrospun using both the

traditional flat-plate collector and our spherical dish and metal array collector, followed by biological evaluation of both scaffold types with INS-1 cells.

ECM functionality is highly regulated by complex cellular interactions with different fibrillar proteins that perform biological activities at the nanoscale dimension [39–42]. Furthermore, numerous reports have demonstrated a positive influence of nanofibrous biomaterial structures on cellular activity [15,43]. Hence, the scaffold parameters designed for this study were specifically chosen to create electrospun nanofibers that were similar in scale to native ECM macromolecules. As demonstrated in Figure 3, the majority of fiber diameters in the traditional ePCL scaffolds were between 300–400 nm, while the cotton ball-like ePCL scaffolds displayed fiber morphologies with an approximate diameter of 500 nm. Therefore, both of these were within the typical size range of collagen fiber bundles found in native ECM [44]. Additionally, even with the different parameters (PCL concentration, flow rate, and voltage), the 2D and 3D nanofiber characteristics were similar. However, the overall scaffold morphologies were significantly affected by the collectors: the traditional collector generated a tightly packed fibrous network, while the new collector was able to create an uncompressed, loosely packed, and more porous nanofibrous structure.

While the influence of nanofiber diameters on cellular behavior is well established, the effect of pore sizes is not so clear. For cellular growth and vascularization in bone, pore sizes of >300 μm have been recommended [45], while fibroblasts have been shown to prefer a pore size of 6 – 20 μm [16]. Even though optimal pore size is tissue-specific, a minimum threshold for porosity with interconnectivity throughout is still needed within tissue engineered scaffolds to ensure that localized cells and nutrients have access to the internal environment, thereby creating an ECM-like three dimensional structure. However, traditional electrospinning is not conducive to the simultaneous production of fibers at the nanoscale size with large pore size interconnectivity. Previously, this has resulted in the traditional electrospun scaffolds requiring post-fabrication modifications. However, these modifications typically alter the nanofiber characteristics and scaffold stability [20,21,24,25]. Additionally, previous efforts for modifying electrospun scaffolds have focused on superficial, planar pores, rather than multi-planar pores to allow for increased cellular infiltration. Consequently, this study provides a comparative look at the fabrication and increased benefit of multi-planar pores via our cotton ball-like ePCL scaffolds in relation to superficially porous scaffolds as generated by traditional electrospinning means.

To identify the superficial pore characteristics, we imaged both scaffolds with a scanning electron microscope (SEM). Examining the SEM images in Figure 3, the nanofiber densities in the two scaffolds can be easily differentiated; there were significantly fewer nanofibers occupying the same space in the cotton ball-like ePCL scaffold compared to the traditional ePCL scaffold. Furthermore, the traditional ePCL scaffold consistently displayed pores < 1 μm, while the cotton ball-like ePCL scaffold had a typical pore size between 2 – 5 μm. We believe that the increased pore sizes in the cotton ball-like scaffold will allow cells enough room to deeply infiltrate the scaffold, while still providing the needed interconnectivity to bridge the pores across multiple nanofibers.

While the SEM images analyzed the superficial regions of both electrospun scaffold types, questions still remained about the internal structure and arrangement. Specifically, qualitative analysis of the nanofibrous characteristics deep within the scaffolds were still needed. Addressing this issue, we decided to incubate the ePCL samples in DAPI. When illuminated at a wavelength of 360 nm, the resulting fluorescence was able to clearly show the contours of the nanofibrous morphologies. Thus, we used confocal microscopy under a fluorescent filter to study the morphologies of both scaffold types throughout their thicknesses. As demonstrated in Figure 4, the traditional ePCL scaffold had a very tightly

packed nanofibrous structure, whereas the cotton ball-like ePCL scaffold had a much more open structure throughout its depth. These contrasting nanofiber characteristics demonstrate the effect of the significantly different collector systems used; the spherical dish and metal array collector helped accumulate the nanofibers in an uncompressed manner, which allowed for more separation between subsequent nanofiber layers. Remarkably, the traditional ePCL scaffolds could only be imaged to a depth of ~10 μm, while the cotton ball-like ePCL scaffolds enabled viewing at a depth up to ~35 μm. This indicated that the increased density of the traditional ePCL scaffold prevented the excitation light from the confocal microscope from deeply penetrating the scaffold. Conversely, the less-dense and more porous cotton ball-like ePCL scaffold was more apt to deeper confocal penetration. This stark contrast in confocal microscopy imaging further verifies the advantageous design of the un-dense, loosely packed network structure of the cotton ball-like scaffolds for cellular infiltration compared to the dense, tightly packed nature of traditional scaffolds. To the best of our knowledge, this combination of an uninterrupted network of nanofibers coupled with deep, multi-planar pores in a stable three dimensional structure has never been demonstrated before in an as-spun, unmodified electrospun scaffold.

An ideal tissue engineered scaffold should promote both good cellular attachment and infiltration, and the balanced combination of both is needed to eventually promote whole tissue formation. Achieving this balance in electrospun scaffolds, though, has proven to be elusive. Specifically, traditionally electrospun scaffolds allow cells to attach superficially; however, they do not provide the large pore sizes needed for substantial cellular infiltration [7,19,46]. In addition, current modification techniques to improve infiltration have been found to impede scaffold stability [23,25]. Thus, as described above, we have designed a spherical dish and metal array collector that is capable of successfully combining nanofibrous morphologies with deep pores in a stable cotton ball-like structure. To identify and contrast cellular responses on the traditional and cotton ball-like ePCL scaffolds, we seeded INS-1 cells and studied their infiltration and growth. To evaluate the cellular response, both scaffolds (each with a diameter of 0.5 cm) were seeded with 64,000 cells, which is ~90% confluence on the top surface. This encouraged cell growth to be directed into the scaffold, thereby demonstrating the relative capacity for in-growth within both scaffold types.

INS-1 cells on the traditional ePCL scaffolds did not infiltrate below the most superficial layer, even after 7 days, whereas cells on the cotton ball-like ePCL scaffolds gradually infiltrated deep into the scaffold (Figure 5). On day 1, the INS-1 cells had attached to the surface of the cotton ball-like ePCL scaffold, and their infiltration was limited to the top surface (Figure 5b). By day 3, most of the cells had infiltrated past the superficial threshold (~125 μm), and a few had even infiltrated deep into the scaffold to a depth of ~260 μm (Figure 5d). Furthermore, by day 7, cells were present throughout the scaffold at a depth of ~300 μm from the surface, and the number of cells had increased tremendously, both near the surface and deep within the scaffold (Figure 5f). These promising results correlated directly to the more open, loosely packed network structure shown in Figure 4b, which allowed the cells an easier path for deep infiltration and greater cell proliferation. In contrast, the tightly packed structure of traditional ePCL scaffolds (Figures 4a,c,e,) presents obstructions that limit cell attachment to the top-most surface layer.

Next, the cellular response was qualitatively evaluated, and as shown in Figure 6, cell growth between days 1 and 3 was similar on both the traditional and cotton ball-like ePCL scaffolds. The cell number on the traditional ePCL scaffolds increased to 123.18 ± 6.23 % on day 3 (as normalized to the cell number on day 1), while the cotton ball-like ePCL scaffolds increased to 130.69 ± 25.49 %. The most striking change, though, was observed between days 3 and 7. Over this time, the cell number increased to 137.35 ± 3.14 % on day 7

(as normalized to Day 1) on the traditional ePCL scaffolds, whereas the value for the cotton ball-like ePCL scaffolds jumped to 178.96 ± 37.09 %. These results, combined with the qualitative histology images in Figure 5, strongly demonstrate the influence of the cotton ball-like ePCL scaffold for increasing cellular infiltration and growth. Because of the high initial seeding density, cells on the traditional ePCL scaffolds quickly proliferated to fill the available space on the top surface of the scaffold by day 3, after which the growth rate slowed due to poor cellular infiltration. Hence, there was only ~11% growth between days 3 and 7 on the traditional ePCL scaffold. Meanwhile, the greater thickness and more open, porous nanofibrous network of the cotton ball-like ePCL scaffolds with three dimensionality (Figure 2b) allowed space for continuous cellular infiltration (Figures 5b, 5d, and 5f) and growth throughout, resulting in the number of attached cells increasing ~37% between days 3 and 7. These cumulative data conclusively prove that the cotton ball-like ePCL scaffolds provide a better host environment for cellular infiltration and growth than the traditional ePCL scaffolds.

4. Conclusion

Current electrospinning techniques do not simultaneously provide deep, interconnected pores within a stable, three-dimensional nanofibrous structure. To address this problem, we have developed an electrospinning technique using a dish with an embedded array of metal probes to create a focused accumulation of ePCL nanofibers that assemble together in a cotton ball-like structure. SEM and confocal microscopy showed a more porous and spacious nanofiber scaffold. Histology and quantitative cell growth demonstrated increased cell penetration and proliferation for the cotton ball-like scaffold over the traditional ePCL scaffold. This strategy provides a new solution for overcoming the current challenges facing the electrospinning process and has great potential across a wide range of tissue engineering applications.

Acknowledgments

The authors would like to acknowledge the efforts of Dr Robin Foley for SEM imaging and Shawn Williams and the High Resolution Imaging Facility for confocal imaging. We would also like to thank Patricia Lott at the Histomorphometry and Molecular Analyses core facility at the Center for Metabolic Bone Disease and Carlos A Carmona Moran for their assistance in histology. This work was funded by the Wallace H. Coulter Foundation, UAB Diabetes Research Training Center Pilot Grant, Innovation Award from the American Diabetes Association, and NSF CAREER (CBET-0952974) for H.-W.J. Additional financial support is acknowledged from the NIH T32 predoctoral training grant (NIBIB #EB004312-01) and Ruth L. Kirschstein National Research Service Award Individual Fellowship (1F31DE021286-01) for J.M.A., along with the AHA Greater Southeast Affiliate Predoctoral Fellowship Program (10PRE3500024) for A.A.

References

[1]. Gupta D, Venugopal J, Mitra S, Dev VG, Ramakrishna S. Nanostructured biocomposite substrates by electrospinning and electrospraying for the mineralization of osteoblasts. Biomaterials 2009;30(11):2085–94. [PubMed: 19167752]

[2]. Shin M, Yoshimoto H, Vacanti J. In vivo bone tissue engineering using mesenchymal stem cells on a novel electrospun nanofibrous scaffold. Tissue Eng 2004;10(1–2):33–41. [PubMed: 15009928]

[3]. Zhang Y, Venugopal J, El-Turki A, Tamakrishna S, Su B, Lim C. Electrospun biomimetic nanocomposite nanofibers of hydroxyapatite/chitosan for bone tissue engineering. Biomaterials 2008;29(32):4314–22. [PubMed: 18715637]

[4]. Tortelli F, Cancedda R. Three-Dimensional Cultures of Osteogenic and Chondrogenic Cells: A Tissue Engineering Approach to Mimic Bone and Cartilage In Vitro. Eur Cells Mater 2009;17:1–14.

[5]. Chen J, Xu J, Wang A, Zheng M. Scaffolds for tendon and ligament repair: review of the efficacy of commercial products. Expert Rev Med Devic 2009;6(1):61–73.

[6]. Kumbar S, Nukavarapu S, James R, Nair L, Laurencin C. Electrospun poly(lactic acid-co-glycolic acid) scaffolds for skin tissue engineering. Biomaterials 2008;29(30):4100–7. [PubMed: 18639927]

[7]. Zhu X, Cui W, Li X, Jin Y. Electrospun fibrous mats with high porosity as potential scaffolds for skin tissue engineering. Biomacromolecules 2008;9(7):1795–801. [PubMed: 18578495]

[8]. Prabhakaran M, Venugopal J, Ramakrishna S. Mesenchymal stem cell differentiation to neuronal cells on electrospun nanofibrous substrates for nerve tissue engineering. Biomaterials 2009;30(28):4996–5003. [PubMed: 19539369]

[9]. Feng Z, Chu X, Huang N, Wang T, Wang Y, Shi X, et al. The effect of nanofibrous galactosylated chitosan scaffolds on the formation of rat primary hepatocyte aggregates and the maintenance of liver function. Biomaterials 2009;30(14):2753–63. [PubMed: 19232710]

[10]. Venugopal J, Ma LL, Yong T, Ramakrishna S. In vitro study of smooth muscle cells on polycaprolactone and collagen nanofibrous matrices. Cell Biol Int 2005;29(10):861–7. [PubMed: 16153863]

[11]. Jun I, Jeong S, Shin H. The stimulation of myoblast differentiation by electrically conductive sub-micron fibers. Biomaterials 2009;30(11):2038–47. [PubMed: 19147222]

[12]. Shin M, Ishii O, Sueda T, Vacanti JP. Contractile cardiac grafts using a novel nanofibrous mesh. Biomaterials 2004;25(17):3717–23. [PubMed: 15020147]

[13]. Wray L, Orwin E. Recreating the microenvironment of the native cornea for tissue engineering applications. Tissue Eng Pt A 2009;15(7):1463–72.

[14]. Pham QP, Sharma U, Mikos AG. Electrospinning of Polymeric Nanofibers for Tissue Engineering Applications: A Review. Tissue Eng 2006;12(5):1197–211. [PubMed: 16771634]

[15]. Li WJ, Jiang YJ, Tuan RS. Chondrocyte Phenotype in Engineered Fibrous Matrix is Regulated by Fiber Size. Tissue Eng 2006;17(7):1775–85. [PubMed: 16889508]

[16]. Lowery J, Datta N, Rutledge G. Effect of fiber diameter, pore size and seeding method on growth of human dermal fibroblasts in electrospun poly(epsilon-caprolactone) fibrous mats. Biomaterials 2010;31(2):491–504. [PubMed: 19822363]

[17]. Patlolla A, Collins G, Arinzeh TL. Solvent-dependent properties of electrospun fibrous composites for bone tissue regeneration. Acta Biomater 2010;6(1):90–101. [PubMed: 19631769]

[18]. Eichhorn SJ, Sampson WW. Statistical geometry of pores and statistics of porous nanofibrous assemblies. J R Soc Interface 2005;2(4):309–18. [PubMed: 16849188]

[19]. Thorvaldsson A, Stenhamre H, Gatenholm P, Walkenstrom P. Electrospinning of highly porous scaffolds for cartilage regeneration. Biomacromolecules 2008;9(3):1044–9. [PubMed: 18260633]

[20]. Kim T, Chung H, Park T. Macroporous and nanofibrous hyaluronic acid/collagen hybrid scaffold fabricated by concurrent electrospinning and deposition/leaching of salt particles. Acta Biomaterialia 2008;4(6):1611–9. [PubMed: 18640884]

[21]. Nam J, Huang Y, Agarwai S, Lannutti J. Improved Cellular Infiltration in Electrospun Fiber via Engineered Porosity. Tissue Eng 2007;13(9):2249–57. [PubMed: 17536926]

[22]. Wei H-J, Chen C-H, Lee W-Y, Chiu I, Hwang S-M, Lin W-W, et al. Bioengineered cardiac patch constructed from multilayered mesenchymal stem cells for myocardial repair. Biomaterials 2008;29(26):3547–56. [PubMed: 18538386]

[23]. Yang X, Shah JD, Wang H. Nanofiber Enabled Layer-by-Layer Approach Toward Three-Dimensional Tissue Formation. Tissue Eng Pt A 2009;15(4):945–56.

[24]. Baker BM, Gee AO, Metter RB, Nathan AS, Marklein RA, Burdick JA, et al. The potential to improve cell infiltration in composite fiber-aligned electrospun scaffolds by the selective removal of sacrificial fibers. Biomaterials 2008;29(15):2348–58. [PubMed: 18313138]

[25]. Ekaputra A, Prestwich G, Cool S, Hutmacher D. Combining Electrospun Scaffolds with Electrosprayed Hydrogels Leads to Three-Dimensional Cellularization of Hybrid Constructs. Biomacromolecules 2008;9(8):2097–103. [PubMed: 18646822]

[26]. Baker SC, Atkin N, Gunning PA, Granville N, Wilson K, Wilson D, Southgate J. Characterisation of electrospun polystyrene scaffolds for three-dimensional in vitro biological studies. Biomaterials 2006;27(16):3136–46. [PubMed: 16473404]

[27]. Tambralli A, Blakeney B, Anderson J, Kushwaha M, Andukuri A, Dean D, et al. A hybrid biomimetic scaffold composed of electrospun polycaprolactone nanofibers and self-assembled peptide amphiphile nanofibers. Biofabrication 2009;1(2):025001. [PubMed: 20811101]

[28]. Murugan R, Ramakrishna S. Design strategies of tissue engineering scaffolds with controlled fiber orientation. Tissue Eng 2007;13(8):1845–66. [PubMed: 17518727]

[29]. Yang S, Leong KF, Du Z, Chua CK. The design of scaffolds for use in tissue engineering: I. Traditional Factors. Tissue Eng 2001;7(6):679–89. [PubMed: 11749726]

[30]. Choi JS, Lee SJ, Chris GJ, Atala A, Yoo JJ. The influence of electrospun aligned poly(epsilon-caprolactone)/collagen nanofiber meshes on the formation of self-aligned skeletal muscle myotubes. Biomaterials 2008;29(19):2899–906. [PubMed: 18400295]

[31]. Li WJ, Danielson KG, Alexander PG, Tuan RS. Biological response of chondrocytes cultured in three-dimensional nanofibrous poly(epsilon-caprolactone) scaffolds. J Biomed Mater Res A 2003;67(4):1105–14. [PubMed: 14624495]

[32]. Li WJ, Tuli R, Okafor C, Derfoul A, Danielson KG, Hall DJ, et al. A three-dimensional nanofibrous scaffold for cartilage tissue engineering using human mesenchymal stem cells. Biomaterials 2005;26(6):599–609. [PubMed: 15282138]

[33]. Ma Z, He W, Yong T, Ramakrishna S. Grafting of gelatin on electrospun poly(caprolactone) nanofibers to improve endothelial cell spreading and proliferation and to control cell orientation. Tissue Eng 2005;11(7–8):1149–58. [PubMed: 16144451]

[34]. Yoshimoto H, Shin YM, Terai H, Vacanti JP. A biodegradable nanofiber scaffold by electrospinning and its potential for bone tissue engineering. Biomaterials 2003;24(12):2077–82. [PubMed: 12628828]

[35]. Zhang YZ, Venugopal J, Huang ZM, Lim CT, Ramakrishna S. Characterization of the surface biocompatibility of the electrospun PCL-collagen nanofibers using fibroblasts. Biomacromolecules 2005;6(5):2583–9. [PubMed: 16153095]

[36]. Asfari M, Janjic D, Meda P, Li G, Halban PA, Wollheim CB. Establishment of 2-mercaptoethanol-dependent differentiated insulin-secreting cell lines. Endocrinology 1992;130(1):167–78. [PubMed: 1370150]

[37]. Hohmeier HE, Mulder H, Chen G, Henkel-Rieger R, Prentki M, Newgard CB. Isolation of INS-1-derived cell lines with robust ATP-sensitive K+ channel-dependent and -independent glucose-stimulated insulin secretion. Diabetes 2000;49(3):424–30. [PubMed: 10868964]

[38]. Yang S, Fransson U, Fagerhus L, Holst LS, Hohmeier HE, Renstrom R, et al. Enhanced cAMP protein kinase A signaling determines improved insulin secretion in a clonal insulin-producing deta-cell line (INS-1 832/13). Mol Endocrinol 2004;18(9):2312–20. [PubMed: 15166255]

[39]. Daley WP, Peters SB, Larsen M. Extracellular matrix dynamics in development and regenerative medicine. J Cell Sci 2008;121(Pt 3):255–64. [PubMed: 18216330]

[40]. Hubbell JA. Materials as morphogenetic guides in tissue engineering. Curr Opin Biotechnol 2003;14(5):551–8. [PubMed: 14580588]

[41]. Kleinman HK, Philip D, Hoffman MP. Role of the extracellular matrix in morphogenesis. Curr Opin Biotechnol 2003;14(5):526–32. [PubMed: 14580584]

[42]. Streuli C. Extracellular matrix remodeling and cellular differentiation. Curr Opin Cell Biol 1999;11(5):643–40.

[43]. Kwon IK, Kidoaki S, Matsuda T. Electrospun nano- to microfiber fabrics made of biodegradable copolyesters: structural characteristics, mechanical properties and cell adhesion potential. Biomaterials 2005;26(18):3929–39. [PubMed: 15626440]

[44]. Elsdale T, Bard J. Collagen substrata for studies on cell behavior. J Cell Biol 1972;54(3):626–37. [PubMed: 4339818]

[45]. Karageorgiou V, Kaplan D. Porosity of 3D biomaterial scaffolds and osteogenesis. Biomaterials 2005;26(27):5474–91. [PubMed: 15860204]

[46]. Telemeco TA, Ayres C, Bowlin GL, Wnek GE, Boland ED, Cohen N, et al. Regulation of cellular infiltration into tissue engineering scaffolds composed of submicron diameter fibrils produced by electrospinning. Acta Biomater 2005;1(4):377–85. [PubMed: 16701819]

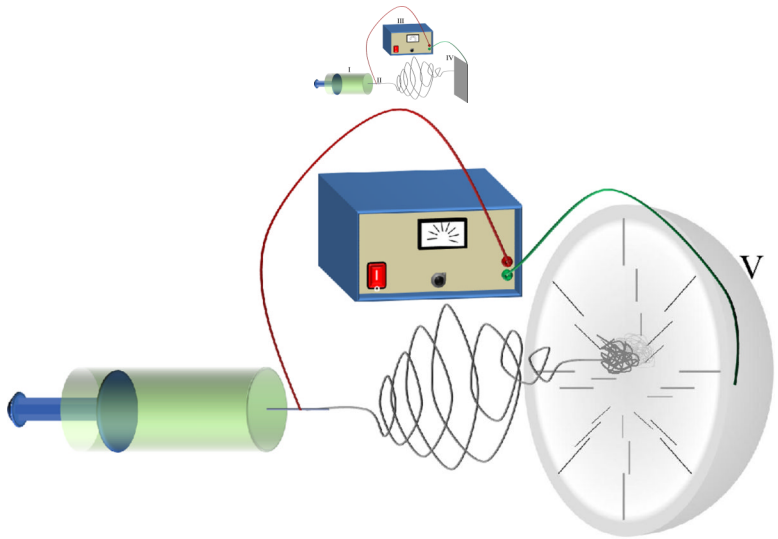

Figure 1.

(a) Scheme for traditional electrospinning. (b) Scheme for creating a cotton ball-like electrospun scaffold using spherical dish and metal array. The PCL solution in the syringe (I) is ejected from the syringe nozzle (II). The solution is attracted to the grounded collectors by the voltage difference generated by (III). In Figure 1a. the electrospun PCL nanofibers accumulate as tightly packed layers on the traditional flat-plate collector (IV), and in Figure 1b, the spherical dish collector (V) allows nanofibers to accumulate in a structure resembling a cotton ball.

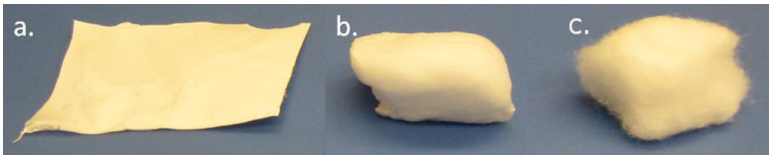

Figure 2.
(a) A traditional ePCL scaffold with a flat, two-dimensional structure with no depth for the traditional scaffolds. (b) A cotton ball-like ePCL scaffold shows with a fluffy, three-dimensional structure of the scaffolds. (c) A cotton ball, which illustrates the relative shape and density of the electrospun nanofibers.

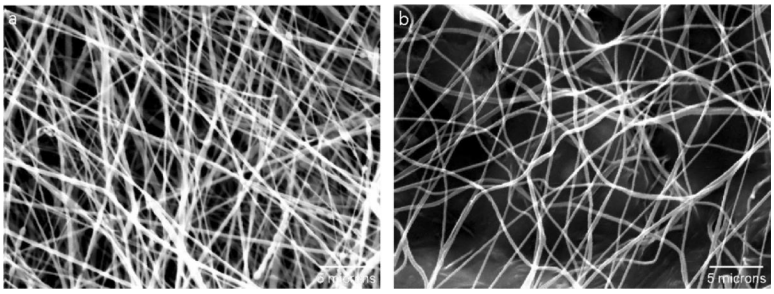

Figure 3.
(a) SEM image of traditional ePCL nanofibers collected using a flat sheet with nanofiber diameters between 300–400 nm and pore sizes < 1 μm. (b) SEM image of cotton ball-like ePCL nanofibers collected using the spherical dish and metal array collector with nanofiber diameters around 500 nm and pore sizes between 2–5 μm. For both images, magnification is 5000× and scale bars = 5 μm.

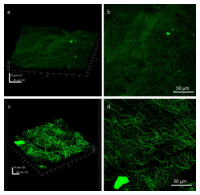

Figure 4.
Confocal microscopy images of (a) three-dimensional rendering of a traditional ePCL scaffold and (b) two-dimensional projection of a traditional ePCL scaffold show a tightly packed nanofibrous structure. In contrast, the confocal microscope images of the (c) three-dimensional rendering of a cotton ball-like ePCL scaffold and (d) two-dimensional projection of a cotton ball-like ePCL scaffold show an un-dense, loosely packed network structure throughout its depth.

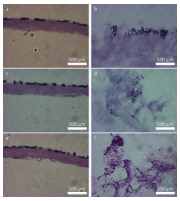

Figure 5.
Images of H&E stained sections of traditional ePCL scaffolds seeded with INS-1 cells after (a) 1 day, (c) 3 days, and (e) 7 days show that cellular infiltration is limited to the top layers of the scaffolds, even after 7 days. Images of H&E stained sections of cotton ball-like ePCL scaffolds after (b) 1 day, (d) 3 days, and (f) 7 days show that there is a progressive infiltration and growth into the scaffolds throughout the 7 days. For all images, section thicknesses = 20 μm, magnification = 20×, and scale bars = 100 μm.

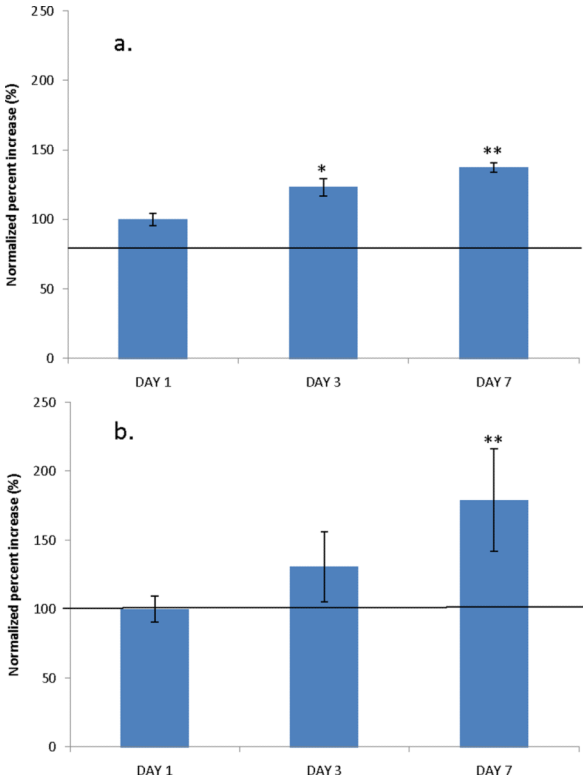

Figure 6.

Normalized INS-1 cells growth on (a) the traditional ePCL scaffolds shows a gradual increase in cell number until 7 days: whereas, on (b) the cotton ball-like ePCL scaffolds a dramatic increase in cell number can be seen at Day 7. In both images, the horizontal normalization line has been included to better illustrate the difference in cell growth. *Cell number at Day 3 is significantly greater than at Day 1 ($p<0.05$). **Cell number at Day 7 is significantly greater than at Days 1 and 3 ($p<0.05$). Error bars represent means ± standard deviation. n=4